3.3 Analysis Coordinator

1. Introduction

In this report we outline the activities of the Analysis Coordinator during 2015. The main activities were analysis of the ITRF2014 extended model presentation of post-seismic deformation after large earthquakes and a comparison of recent diurnal and semi-diurnal EOP models with the IERS Conventions (2010).

2. Analysis of ITRF2014 post-seismic parameterization

The ITRF2014 reference frame, as generated by IGN, contains parametric fits to earthquake post seismic motions as an alternative to the piece-wise linear functions that had been used in earlier ITRFs. Two parametric forms are used:

$$p(t) = A\left(1 - e^{-\frac{t}{T_e}}\right) \quad \text{Exponential}$$

$$p(t) = A\ln(1 + \frac{t}{T_l}) \quad \text{Logarithmic}$$

where $P(t)$ is a position evolution with time in topocentric North, East, Up direction, T_e is an exponential decay time, and T_l is a logarithmic decay time. One earthquake can have different combinations of exponential and logarithmic terms with different time constants and different numbers of terms between each of the topocentric components at a site. In this report we examine the long term implications of these types of models applied in ITRF2014.

We start by looking at two metrics of these models. The exponential model decays to a steady state such that after a finite duration the total residual motion remaining can be calculated. We denote t_{1mm} at the duration after an earthquake until the total remaining postseismic deformation is less than 1 mm:

$$t_{1mm} = -T_e\ln(\frac{1\text{mm}}{A})$$

where the exponent amplitude is in units of mm. For the logarithmic function there is no corresponding limit (i.e., log will go to infinity as time goes to infinity) and for log decay we use the time until instantaneous velocity due to the log is less than specified amount. The log velocity is given by

$$\frac{dp(t)}{dt} = \frac{A}{\left(1 + \frac{t}{T_l}\right)T_l} \approx A/t$$

In the figures below, we show the time until the log velocity is less than 0.1 mm/yr. Our general interest is in exploring the duration of data that would need to be deleted if the post-seismic curvature terms were ignored and the earthquake was modeled as simply an offset and data processing resumed only after the post-seismic

terms had “decayed” away. For many of the earthquakes that have effected GPS stations, waiting for postseismic signals to “decay away” is not a viable option.

In Figures 1 and 2 we give examples of the impact of the post-seismic motions of two GPS sites affected by large earthquakes. We see here how large these effects can be with the response at Tsukuba being large enough that the postseismic motions for all sites in this region could extend for many hundreds of years.

A large number of GPS stations in ITRF2014 are effected by post-seismic motion i.e., site with an exponential or logarithmic terms in model parameterization in ITRF2014. In all, 17% of IGS sites in ITRF2014 have at least one post-seismic term in their co-ordinate evolution. Figure 3 shows the time history of the number of GPS sites effected by earthquakes. In general, there are a few sites per year with the peak number being the Mw 9.1 Tohuko

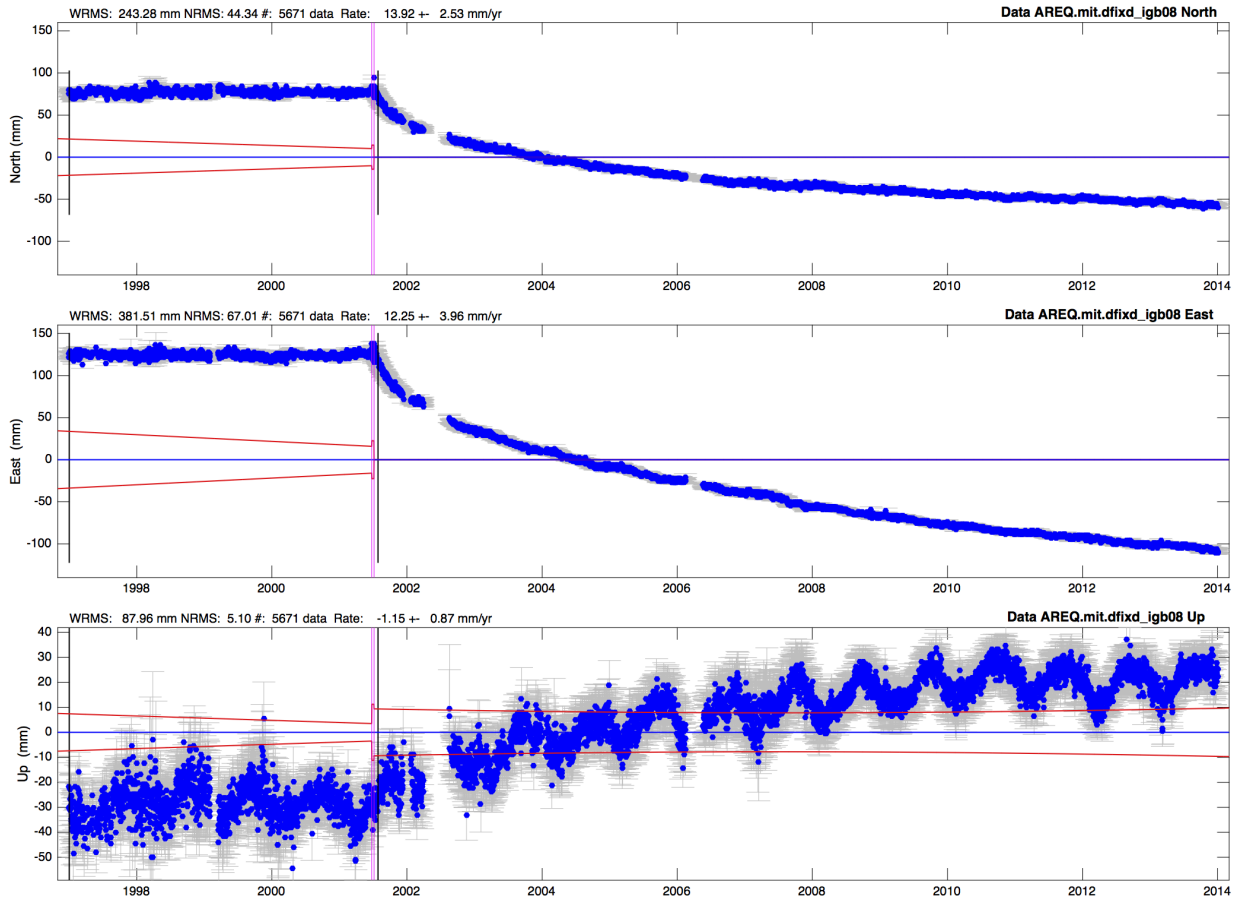

Fig. 1: Residuals to North (top), East (middle) and Up (bottom) position estimates for AREQ (Arequipa, Peru) after removing a linear trend based on data prior to the June 23, 2001 earthquake and the coseismic offset. The post seismic motion from the June 23 and July 7 earthquakes are modeled with exponential decay terms with time constants up to 3162 days. Even a decade after the events the effects of post-seismic motion is still evident.

earthquake in 2011 that generated postseismic motions at 17 GPS sites in the region around Japan (see Figure 5 as well).

We can summarize the effects of the postseismic terms in ITRF2014 by examining the histogram of the duration of time needed for the postseismic terms to becoming negligible. Figure 4 shows these durations based on the ITRF2014 model fits. For the exponential decay we use the time until the remaining post-seismic motion is less than 1.0 mm and for the logarithmic terms, until the instantaneous velocity contribution is less than 0.1 mm/yr (see equations above). For the exponential decay model, the duration times can reach 50 years while for the logarithmic terms the duration is much longer and can reach 2500 years (if the logarithmic is correct).

The global impact of the postseismic terms can be been in Figure 5 where the GPS network is shown (red dots) with those sites that

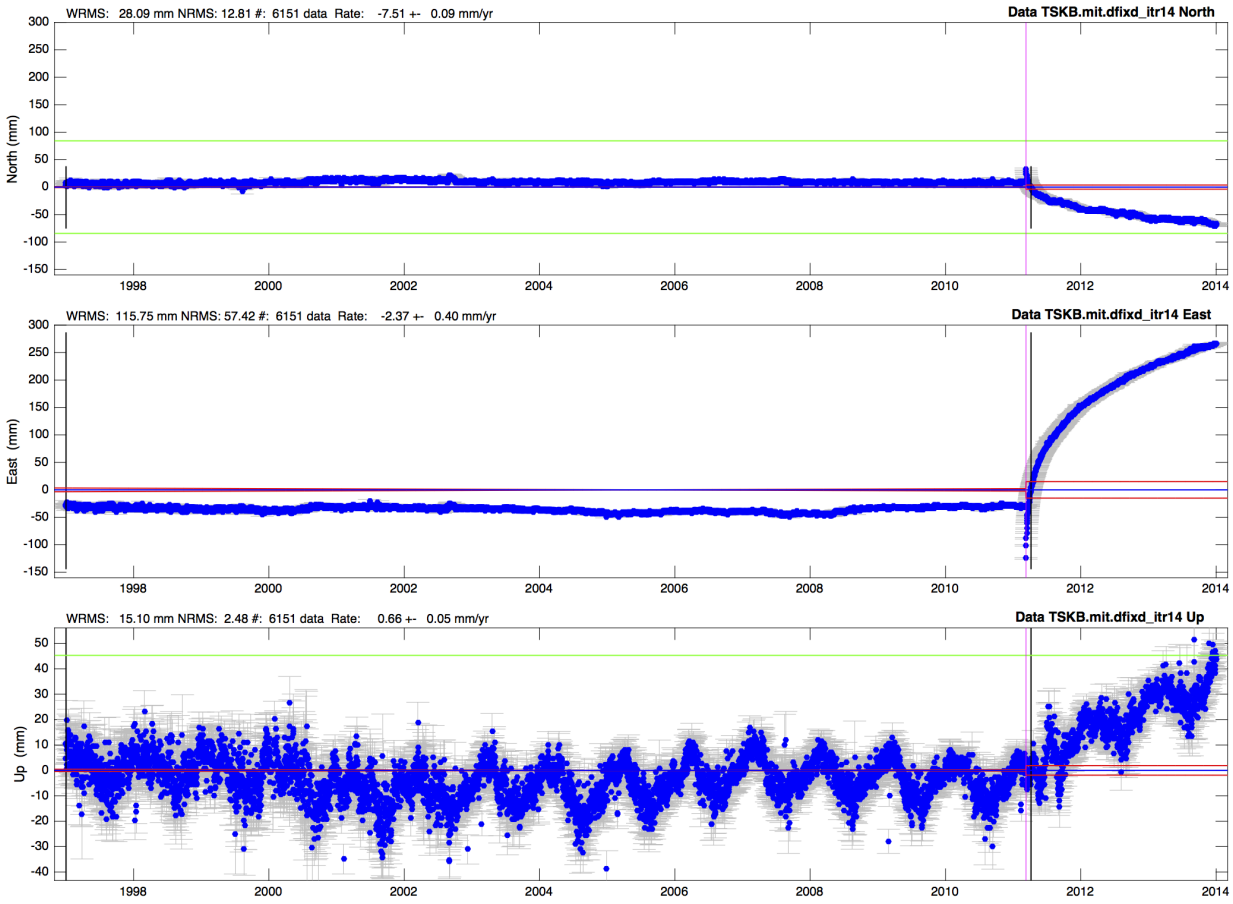

Fig. 2: Residuals to North (top), East (middle) and Up (bottom) position estimates for TSKB (Tsukuba, Japan) after removing a linear trend based on data prior to the March 11, 2011 earthquake and the coseismic offset. The postseismic motion for this earthquake is modeled as combination of log and exponential terms. The amplitude of the log term in the estimates is such that it will be over 500 years before the east velocity returns to its pre-event rate if the log model is correct.

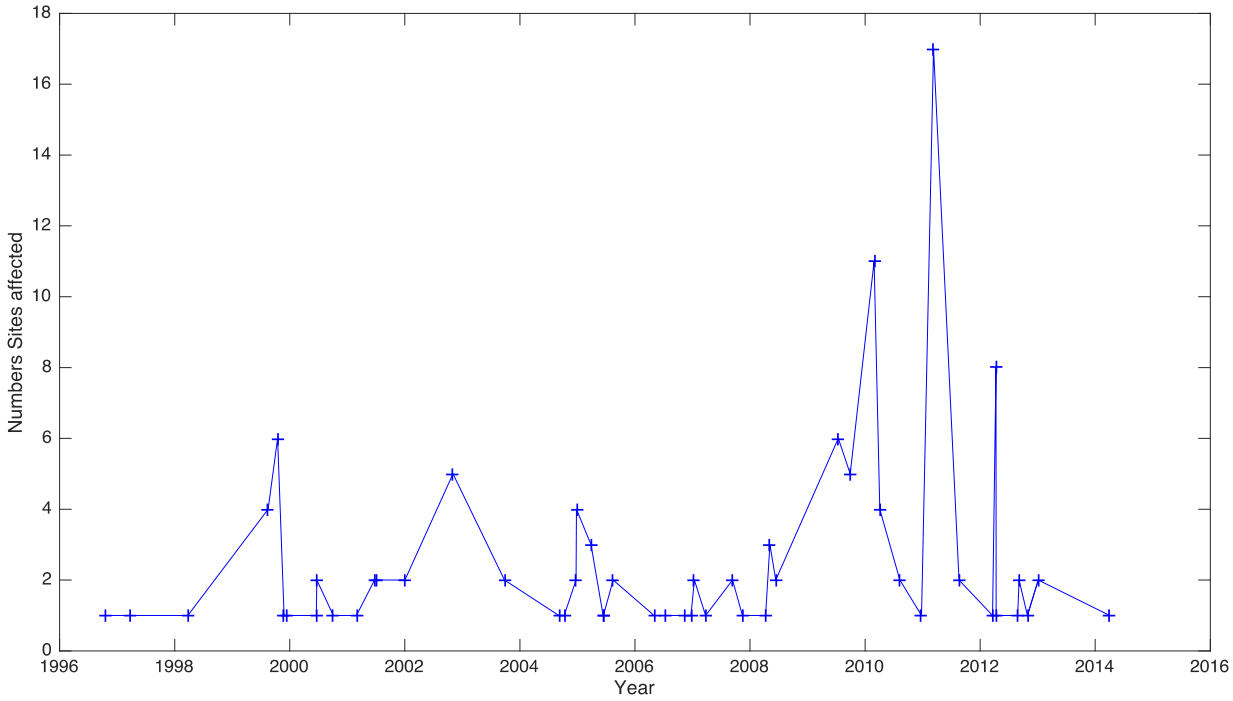

Fig. 3: Count of the number of GPS stations with postseismic terms as a function of time. The largest event is the March 11, 2011 Tohoku magnitude 9.1 earthquake.

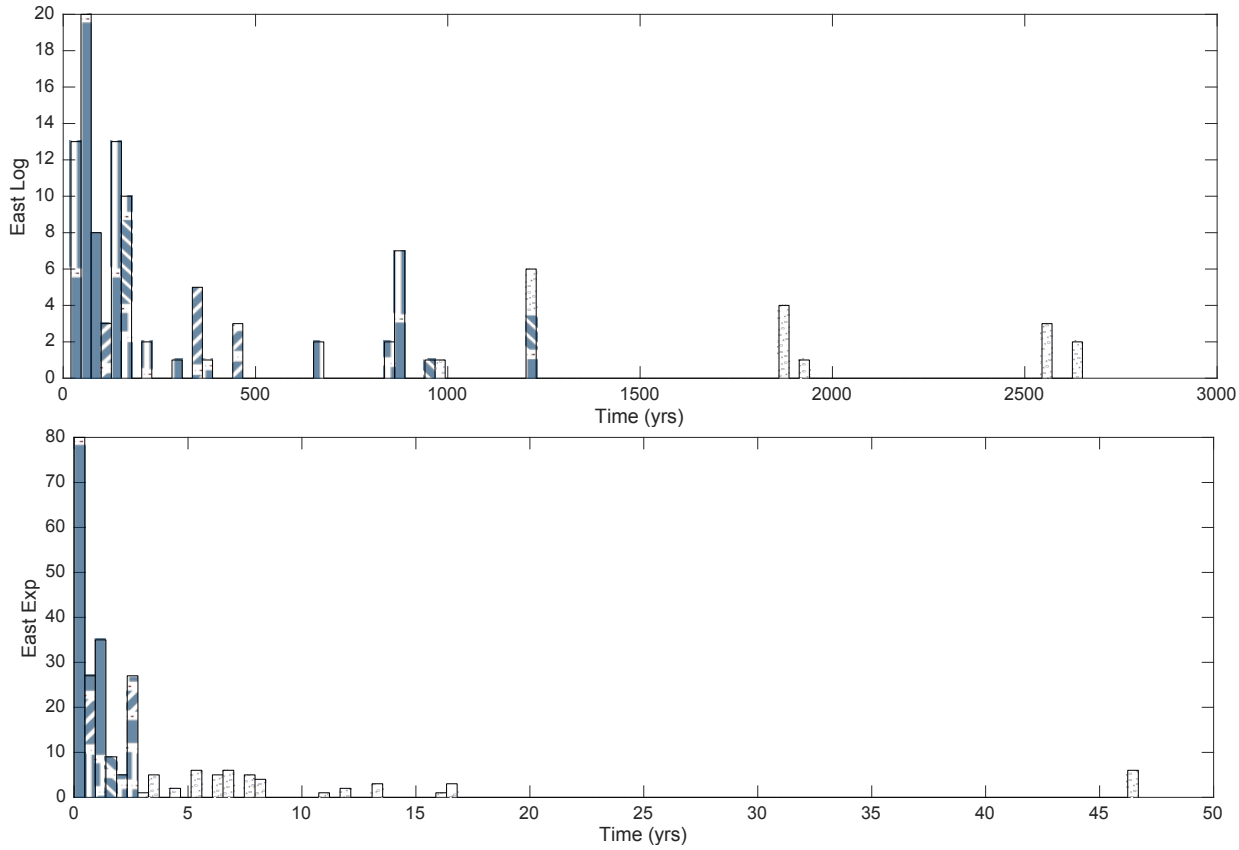

Fig. 4: Histograms of the time intervals needed for postseismic signals to reach negligible levels (0.1 mm/yr for logarithmic and 1 mm for exponential models). The top plot is log terms in ITRF2014 and the bottom plot for exponential terms. See text for discussion.

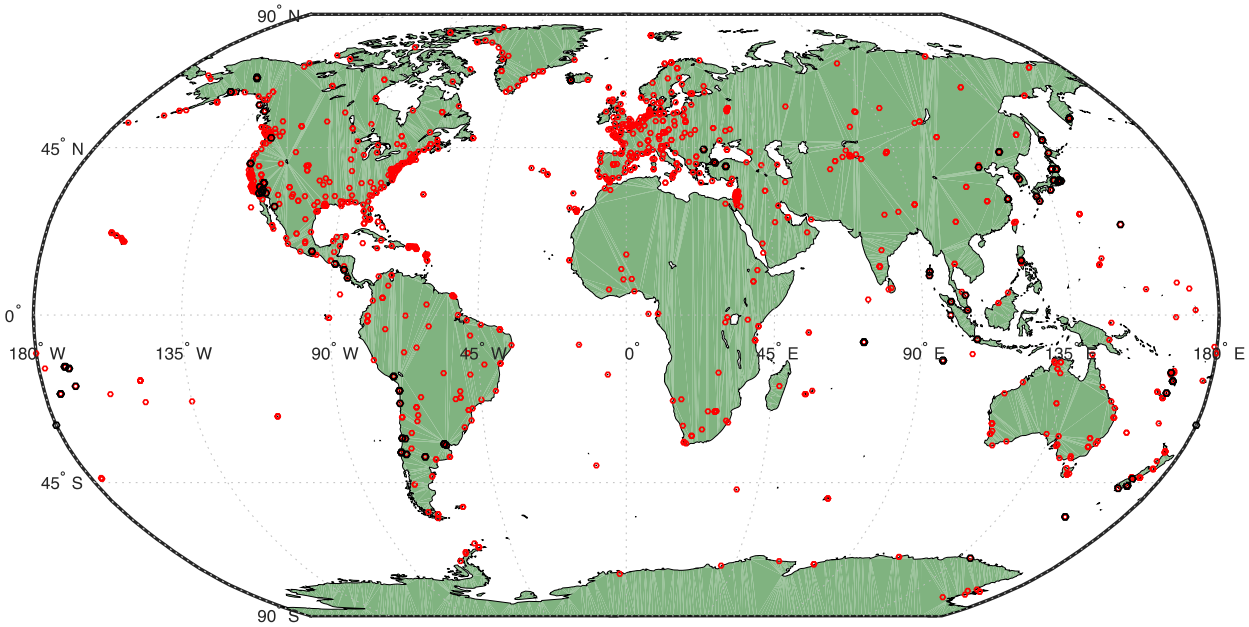

Fig. 5: Distribution of GPS sites in ITRF2014. Red dots are GPS sites and black dots are those stations with post-seismic parameterizations. Approximately 17% of the global network needs postseismic terms.

have post-seismic parametrizations (black). Approximately 17% of sites are affected by postseismic phenomena although this number is probably underestimated. As can be seen in the figure, there are regions of the world where red (un-affected) and black (affected) are interspersed. This occurs because red sites in these regions have no data after the earthquake(s) that results in postseismic deformation at the nearby sites. In the future, this might introduce problems if GPS sites are re-established in these regions because these sites might be undergoing significant post-seismic motions but this will not be apparent because there was no data from the site in the interval immediately after the earthquake.

3. Analysis of diurnal and semidiurnal EOP models

We compared several different up-to-date sub-daily EOP models with the IERS standard model (IERS 2010). The models compared are (the roman numbers are used to refer to the models below).

(i) the diurnal and semidiurnal EOP model determined based on ~35 years VLBI observation by John Gipson.

(ii) the predicted diurnal and semidiurnal EOP variation based on the GOT4.7 ocean tide model, which is the new version of Richard Ray's tide models and has been derived from TOPEX/Poseidon, Jason-1, ERS and GFO altimetry satellites [*Egbert and Erofeeva*, 2002].

(iii) the predicted diurnal and semidiurnal EOP model based on the TPXO.7.1 model, which is computed based on inverse theory using tide gauge and TOPEX/Poseidon data.

(iv) the sub-daily EOP model determined by combining 13-year (1994~2007) GPS and VLBI observations [*Artz et al.,* 2012].

Details about the altimeter satellite tidal models can be found at <https://www.esr.org/polar_tide_models/Model_TPXO71.html>.

We compute the sub-daily EOP for the interval between 1994 and 2015 based on these models. Following tables summarizes the statistics of the differences between these optional models and the current IERS standard model and between the models. Table 1 gives the RMS differences between the four models above and the IERS 2010 model. Table 2 compared the models with each other.

Table 1: Statistics of the differences between the alternative sub-daily EOP models and the IERS standard model during 1994/1/1 – 2014/12/31. The sampling rate of the model is 1 sample per 3 hours, i.e. 8 samples per day. The models are I Gipson; II GOT4.7; III TPXO.71.; IV Artz et al. [2012]. Values in red are the smallest values.

Component	Model I	Model II	Model III	Model IV
Δx [mas]	0.037	0.053	0.043	0.030
Δy [mas]	0.042	0.050	0.045	0.031
Δut1 [μs]	2.544	4.700	1.872	2.782

Table 2: Statistics of the differences among the four sub-daily EOP models during 1994/1/1 – 2014/12/31. The sampling rate of the model is 1 sample per 3 hours, i.e. 8 samples per day. See Table 1 for model names.

Δx [mas]	Model I	Model II	Model III	Model IV
Model I	0	0.0470	0.0285	0.0255
Model II	0.0470	0	0.0369	0.0480
Model III	0.0285	0.0369	0	0.0348
Model IV	0.0255	0.0480	0.0348	0

Δy [mas]	Model I	Model II	Model III	Model IV
Model I	0	0.0425	0.0313	0.0291
Model II	0.0425	0	0.0330	0.0432
Model III	0.0313	0.0330	0	0.0332
Model IV	0.0291	0.0432	0.0332	0

Δut1 [μs]	Model I	Model II	Model III	Model IV
Model I	0	4.7850	2.1873	2.3333
Model II	4.7850	0	4.4478	5.0760
Model III	2.1873	4.4478	0	3.1448
Model IV	2.3333	5.0760	3.1448	0

The discrepancies between these models and current IERS standard model reflect either model improvement or mis-modeling in sub-daily EOP variations. The differences between the newer models are similar in magnitude to the difference to the IERS conventions model and it is not clear which if any would provide an improvement over the IERS model. Models I and IV, both based on geodetic estimates, with Model I being pure VLBI while Model IV combines both VLBI and GPS match the best in polar motion but not in UT1.

References

Artz, T., L. Bernhard, A. Nothnagel, P. Steigenberger and S. Tesmer, Methodology for the combination of sub-daily earth rotation from GPS and VLBI observations. *Journal of Geodesy 86*, 221–239, 2012.

Egbert, G. D. and Erofeeva, L. Efficient inverse modeling of barotropic ocean tides. *Journal of Atmospheric and Oceanic Technology 19*, 183–204, 2002.

Thomas Herring